

Novel Synthetic Strategy for Developing an Isospecific Unbridged Metallocene System for Propylene Polymerization

Seong Kyun Kim, Hwa Kyu Kim, Min Hyung Lee, Seung Woong Yoon, and Youngkyu Do*^[a]

Abstract: New unbridged zirconocenes functionalized with a Lewis base, $[[1-(E-C_6H_4)-3,4-Me_2C_5H_2]_2ZrCl_2]$ ($E = p-NMe_2$ (**3**); $p-OMe$ (**4**); $p-SMe$ (**5**)) were prepared and their propylene polymerization behavior was examined. Under methylaluminoxane (MAO) activation at atmospheric monomer pressure, these complexes afford mixtures of polymers exhibiting multimelting transition temperatures and broad molecular weight distribution, whereas they produce completely atactic polypropylenes under $[Ph_3C][B(C_6F_5)_4]$ activation. Stepwise solvent extraction of

the polymer mixtures reveals that the polymers consist of amorphous, moderately isotactic, as well as, highly isotactic portions and the weight ratio of each portion is dependent upon reaction temperature. The generation of rigid *rac*-like cationic active species in situ by the interaction between basic sites of catalysts and acidic sites of the $[Me-MAO]^-$ counter anion is consid-

ered to be the origin of the observed isospecificity. Further investigation of bulk polymerization in liquid propylene shows not only a considerable increase of the isotactic portion of the obtained polypropylenes but also apparent isospecificity of **4** and **5**/MAO systems even at high temperature. Variation of the Lewis basic center leads to a dramatic change in stereoselectivity of the catalyst in the decreasing order of $3 > 4 \gg 5$, in spite of their structural similarity.

Keywords: isotactic polypropylene • Lewis bases • metallocenes • polymerization • zirconium

Introduction

Single-site catalytic systems based on organometallic complexes have been extensively developed in the field of olefin polymerization during the last two decades to optimize polymer properties, leading to the establishment of the relationship between the nature of catalytic systems and the properties of the resulting polymers, and thereby providing various opportunities to tailor the polymer properties.^[1–10] Among various classes of catalysts, Group 4 metal complex systems have a unique ability to control molecular weight and the distribution, comonomer incorporation, and stereoregularity of the polymer with high activity in a wide range of olefin polymerizations. The correlation between the coordination

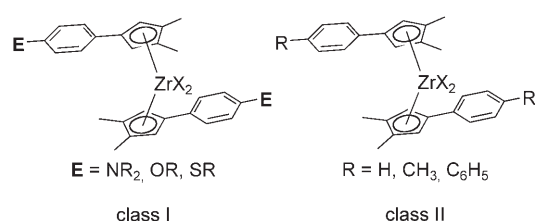
geometry of the catalyst precursors and the stereo- and regiocontrol conforming to an enantiomorphic site-control mechanism in propylene polymerization has been intensively investigated by using chiral *ansa*-metallocene catalysts having a fixed geometry around the metal center.^[3,4,9,10] In this manner, highly isotactic^[11] and syndiotactic polypropylene^[12,13] can be provided by C_2 - and C_s -symmetric *ansa*-metallocenes, respectively.

On the other hand, non *ansa*-metallocenes that are easily accessible synthetically had attracted relatively little attention due to their generally *aspecific* nature until the first report by Erker and co-workers^[14–16] that unbridged metallocene systems having bulky substituents can produce isotactic ($[mmmm] = 0.5–0.7$) polypropylenes. Although the isospecificity could be achieved at a relatively low reaction temperature, this result showed that an unbridged metallocene system is capable of inducing isotactic chain propagation by restricting the rapid ligand rotation. After this significant finding, the “oscillating” $[(2\text{-phenylindenyl})_2ZrCl_2]$ that produces isotactic–atactic, block polypropylene was also reported by Waymouth and co-workers.^[17] The key concept of these papers was to impart isospecific stereocontrol to unbridged metallocene catalysts by introducing hindered

[a] Dr. S. K. Kim, H. K. Kim, Dr. M. H. Lee, S. W. Yoon, Prof. Dr. Y. Do
Department of Chemistry, School of Molecular Science BK-21
Center for Molecular Design and Synthesis
Polyolefin Materials Research Center, College of Natural Science
Korea Advanced Institute of Science and Technology
Daejeon, 305–701 (Korea)
Fax: (+82)42-869-2810
homepage: <http://xray.kaist.ac.kr/>
E-mail: ykdo@kaist.ac.kr

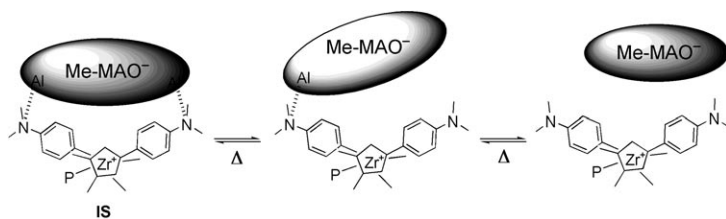
ligand rotation.^[15–26] Although several reports showed that the microstructure of the produced polypropylene strongly depends on the steric and electronic effects of the substituents, as well as on the ion-pair structure of a cationic active center and a counter anion,^[16,20,23,25] in most cases, the unbridged metallocenes afforded atactic polypropylene due to rapid ligand rotation.^[19,27]

When we consider the relative ease of synthesis of unbridged metallocenes compared to that of *ansa*-metallocenes, it is still of great interest to develop unbridged metallocene catalytic systems capable of inducing stereospecific polymerization of propylene. To achieve this goal, we have been pursuing the development of isospecific unbridged metallocene catalytic systems that can be generated in situ during the activation step and have designed a new “class I” of unbridged zirconocenes having Lewis basic substituents.



Whereas zirconocenes having H, Me, or Ph substituents at the *para*-position of the phenylene group (class II) produce completely atactic polypropylene due to the rapid ligand rotation,^[19,27] the Lewis basic sites E in “class I” could interact with $[\text{Me-MAO}]^-$ and thereby generate rigid *rac*-like cationic active species, endowing aspecific unbridged metallocene precatalysts with isospecificity. In this regard, we recently communicated the first example of a dimethylamine-substituted “class I” unbridged zirconocene that exhibits high isoselectivity in propylene polymerization under MAO activation, and also showed that the simultaneous cation–anion pairing and the interactions of Lewis acidic sites in the $[\text{Me-MAO}]^-$ with nitrogen atoms of amine-functionalized unbridged zirconocene cations prevents rapid ligand rotation and favors racemic C_2 -symmetric-like conformers as active species that lead to isospecificity.^[28] (**IS** in Scheme 1)

We expanded our research directions to other Lewis basic heteroatoms such as oxygen and sulfur to address the relationship between the strength of the Lewis acid–base inter-

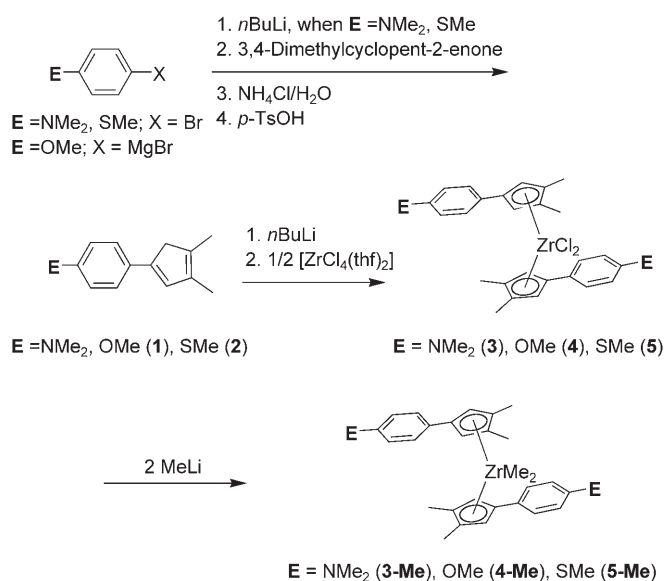


Scheme 1. Isospecific active species (**IS**) and thermal equilibrium with the related species.

actions and the resultant isospecificity in propylene polymerization, including the investigation of the effect of monomer concentration on isospecificity. Herein, the synthesis and the complete set of comparative propylene polymerization studies by using novel Lewis base functionalized zirconocenes, $[\{1-(E-C_6H_4)-3,4-Me_2C_5H_2\}_2ZrCl_2]$ ($E = p\text{-NMe}_2$ (**3**); $p\text{-OMe}$ (**4**); $p\text{-SMe}$ (**5**)) are described.

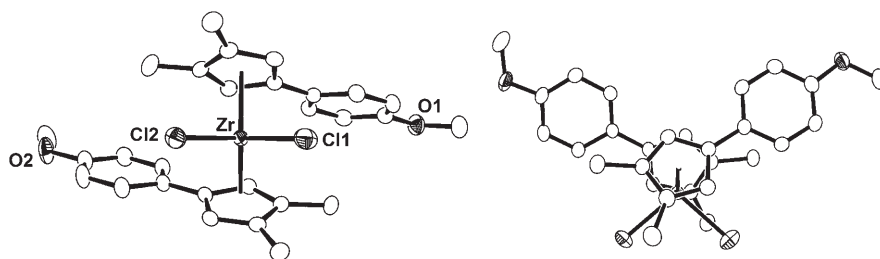
Results and Discussion

Synthesis and characterization: The overall synthetic route of class I unbridged zirconocenes is outlined in Scheme 2. Treatment of *para*-E-bromobenzene ($E = \text{NMe}_2$ and SMe)



Scheme 2. Synthetic route of class I unbridged zirconocenes **3–5**.

with one equivalent of $n\text{BuLi}$ in diethyl ether gave white lithium salts that were further purified and isolated by washing with *n*-hexane. Subsequent reaction of the resulting lithium salts or Grignard reagent ($p\text{-MeO-C}_6\text{H}_4\text{-MgBr}$) with one equivalent of 3,4-dimethylcyclopent-2-enone in THF followed by dehydration with *p*-TsOH in CH_2Cl_2 afforded the desired final ligands, 1-(*p*-E- C_6H_4)-3,4- $\text{Me}_2\text{C}_5\text{H}_3$ ($E = \text{NMe}_2$; OMe (**1**); SMe (**2**)) in good yield. The zirconium complex **3** was synthesized as reported previously,^[28] and the complexes $[\{1-(p\text{-MeOC}_6\text{H}_4)-3,4\text{-Me}_2\text{C}_5\text{H}_2\}_2ZrCl_2]$ (**4**) and $[\{1-(p\text{-MeSC}_6\text{H}_4)-3,4\text{-Me}_2\text{C}_5\text{H}_2\}_2ZrCl_2]$ (**5**) were also prepared straightforwardly by the direct transmetalation of lithium salts of the ligands **1** and **2** with 0.5 equivalents of $[\text{ZrCl}_4(\text{thf})_2]$ in toluene. Dimethylated complexes **3-Me**, **4-Me**, and **5-Me** were prepared by the reaction of **3**, **4**, and **5** with two equivalents of MeLi , respectively. All these complexes are quite soluble in common organic solvents such as toluene and CH_2Cl_2 . According to the molecular structure determination of complex **4**, the C_2 -symmetric, *rac*-like isomer is only seen in the asymmetric unit as similarly ob-

Figure 1. Crystal structure of complex **4** (front and top views).

served in the structure of **3**^[28] (Figure 1). In case of [(2-phenylindenyl)₂ZrCl₂], both *rac*- and *meso*-like isomers are present in the unit cell.^[17] The bonding geometry around the zirconium center, such as bond angles of Cl1–Zr–Cl2 and ring-centroid–Zr–ring-centroid, and bond lengths of Zr–Cl and Zr–ring-centroid are in the range similar to those for other nonbridged zirconocene complexes^[19,29] and very similar to those of **3**^[28] and [(1-(*p*-C₆H₅C₆H₄)-3,4-Me₂C₅H₂)₂ZrCl₂] (BPZr).^[27]

Propylene polymerization: The polymerization of propylene with zirconocenes **3**, **4**, and **5** was achieved at various temperatures of $T_p = 0, 25, 50,$ and 70°C under MAO and [Ph₃C][B(C₆F₅)₄]/TIBA activation at atmospheric monomer pressure and the polymerization results are summarized in Table 1. To compare their polymerization properties, the polymerizations with unfunctionalized “class II”, [(1-(*p*-C₆H₅C₆H₄)-3,4-Me₂C₅H₂)₂ZrCl₂] (BPZr) and the well known isospecific catalyst, *rac*-[Et(Ind)₂ZrCl₂] (EBIZr) were also carried out. When compared with EBIZr/MAO (Table 1, entry 17) under identical polymerization conditions, this “class I” system shows lower catalytic activity but produces

higher-molecular-weight polypropylene. Most of the crude polypropylenes from this system show multimelting transitions (T_m) and a broad molecular-weight distribution (MWD) of $M_w/M_n = 2\text{--}10$ by differential scanning calorimetry (DSC) and gel-permeation chromatography (GPC) (Figure 2) diagrams, respectively, indicating the involvement of multicatalytic active species.^[30] Whereas the polymer from **3**/MAO shows a relatively narrow MWD at 0°C (Table 1, entry 1), the multimodality is clearly seen at higher reaction temperatures (Table 1, entries 2–4). In contrast, the broad MWD from **4**/MAO at 0, 25, and 50°C (Table 1, entries 5–7) becomes much narrower at 70°C (Table 1, entry 8). Unlike the **3**/MAO and **4**/MAO systems, **5**/MAO gave polymers with a narrow MWD at all reaction temperatures (Table 1, entries 9–12). These results indicate that **3**/MAO maintains a multicatalytic active nature even at high temperature, whereas single active species are dominant at high temperature in **4**/MAO and at all temperatures for **5**/MAO. Consistent with the GPC results, DSC diagrams of the polymers from **3**/MAO (Table 1, entries 1–4) and **4**/MAO (Table 1, entries 5–8) also show multimelting transitions with high T_m ($132\text{--}156^\circ\text{C}$). In the case of borate activation, however, **3-Me**/[Ph₃C][B(C₆F₅)₄] (Table 1, entry 13) and **4-Me**/[Ph₃C][B(C₆F₅)₄] (Table 1, entry 14) give completely amorphous polypropylene with low molecular weight and a narrow MWD. Interestingly, **5**/MAO (Table 1, entry 10) and **5-Me**/[Ph₃C][B(C₆F₅)₄] (Table 1, entry 15) show very similar polymerization results under otherwise identical conditions,

Table 1. Propylene polymerization data.^[a]

Entry	Catalyst	Cocatalyst	T_p [$^\circ\text{C}$]	t_p [min]	Yield [g]	Productivity ^[b]	M_w ($\times 10^{-3}$)	M_w/M_n	T_m [$^\circ\text{C}$]	EE-sol wt % ^[c]	EE-insol/C7-sol wt % ^[c]	EE-insol/C7-insol wt % ^[c]
1	3	MAO	0	120	1.02	72.9	227	4.6	156.2	13	21	66
2	3	MAO	25	120	6.24	931	166	10.7	156.6	20	21	59
3	3	MAO	50	120	7.25	2270	32.0	9.5	153.0	50	32	18
4	3	MAO	70	120	3.41	1710	10.1	5.3	141.0	64	22	14
5	4	MAO	0	60	0.588	84.0	259	4.7	151.8	8	33	59
6	4	MAO	25	60	3.91	1170	144	7.3	154.0	19	33	48
7	4	MAO	50	60	6.20	3880	18.8	5.1	132.7	65	30	5
8	4	MAO	70	60	2.31	2310	1.98	2.1	n/o ^[d]	90	10	0
9	5	MAO	0	120	3.71	265	35.9	2.4	n/o	87	11	2
10 ^[b]	5	MAO	25	60	3.88	1160	16.7	2.3	n/o	97	3	0
11	5	MAO	50	60	5.54	3460	5.37	2.2	n/o	100	0	0
12	5	MAO	70	60	3.14	3140	0.90	2.2	n/o	100	0	0
13 ^[d]	3-Me	borate/TIBA	25	120	6.95	1040	15.2	2.1	n/o	100	0	0
14 ^[d]	4-Me	borate/TIBA	25	60	2.69	803	17.4	2.8	n/o	100	0	0
15 ^[d]	5-Me	borate/TIBA	25	60	3.05	910	14.9	2.7	n/o	100	0	0
16 ^[e]	BPZr	MAO	0	60	2.83	404	58.9	1.9	n/o	100	0	0
17 ^[f]	EBIZr	MAO	25	25	12.36	8855	19.1	2.1	128.7	3	97	0

[a] Polymerization conditions: P(propylene) = 1 bar; [Zr] = 5.0 μmol ; [Al]/[Zr] = 1000; solvent = 50 mL of toluene. [b] In units of (Kg of PP)/(mol of Zr)⁻¹h⁻¹[propylene]⁻¹. Propylene solubility has been taken from ref. [31]. [c] EE = diethyl ether; C7 = *n*-heptane. [d] Borate = [Ph₃C][B(C₆F₅)₄]; [B]/[Zr] = 1; TIBA = triisobutylaluminum, [Al]/[Zr] = 200. [e] BPZr = [1-(*p*-C₆H₅C₆H₄)-3,4-Me₂C₅H₂)₂ZrCl₂. [f] EBIZr = *rac*-Et(Ind)₂ZrCl₂. [g] Not observed.

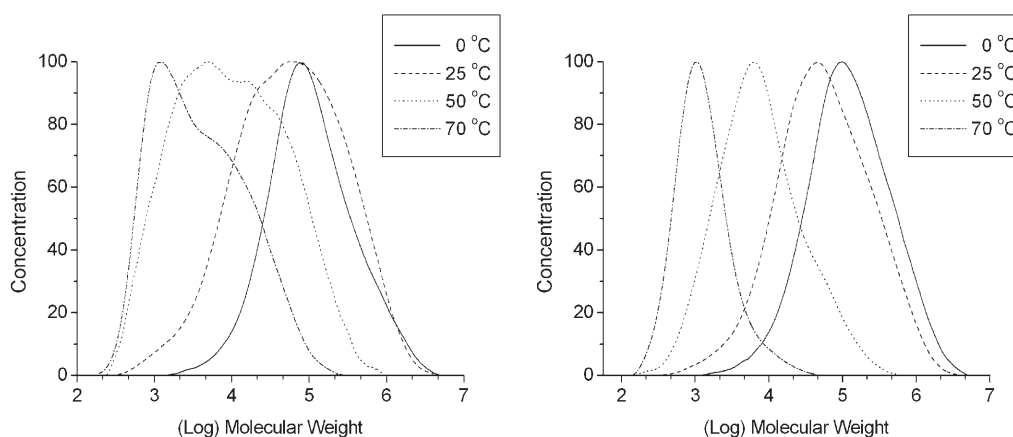


Figure 2. GPC diagram of polypropylenes from entries 1–4 in Table 1 (**3**/MAO at 0, 25, 50, and 70 °C; left) and from entries 5–8 in Table 1 (**4**/MAO at 0, 25, 50, and 70 °C; right).

giving amorphous, low-molecular-weight polypropylene. Thus, it can be seen that the NMe₂- and OMe-substituted zirconocenes **3** and **4** display completely different polymerization behavior upon MAO and [Ph₃C][B(C₆F₅)₄] activation, whereas the polymerization behavior of zirconocene **5** is almost unaffected by the kind of activator at atmospheric monomer pressure.

To obtain more detailed information on the properties of the obtained polypropylenes, the crude polymers were fractionated by a stepwise solvent extraction method into three portions for further analysis: diethyl ether soluble, diethyl ether insoluble and *n*-heptane-soluble, and diethyl ether insoluble and *n*-heptane-insoluble portions.^[32] The *[mmmm]* methyl pentad values and *T_m* of each extracted portion in Table 2 indicate that the foregoing portions correspond to atactic-like, moderately isotactic, and highly isotactic polypropylene, respectively. In the case of the polypropylenes obtained particularly from **3**/MAO (Table 2, entries 1–4) and **4**/MAO (Table 2, entries 5–8), the amount of each portion varies upon polymerization temperature in a way that the *n*-heptane-insoluble portion decreases with increasing temperature, whereas that of the diethyl ether soluble portion increases (Figures 3 and 4). This explains that thermal equilibria between active species exist that are responsible for

Table 2. Detailed analysis of each extracted portion of the polymer samples (EE = diethyl ether, C7 = *n*-heptane).

Entry ^[a]	No.	Extract Portion	wt %	<i>T_m</i> [°C]	<i>M_w</i> (×10 ⁻³)	<i>M_w</i> / <i>M_n</i>	<i>mmmm</i> ^[b] [%]
1	1–1	EE-sol	13	n/o ^[c]	n/d ^[d]	n/d	14
	1–2	C7-sol	21	151.1	85.8	2.5	55
	1–3	C7-insol	66	155.7	337	4.2	85
2	2–1	EE-sol	20	n/o	27.2	5.2	19
	2–2	C7-sol	21	131.8	68.4	4.2	53
	2–3	C7-insol	59	151.3	273	4.3	86
3	3–1	EE-sol	50	n/o	10.7	4.7	17
	3–2	C7-sol	32	146.4	39.4	3.8	67
	3–3	C7-insol	18	148.3	113	2.6	86
4	4–1	EE-sol	64	n/o	5.3	3.4	14
	4–2	C7-sol	22	127.3	17.8	2.6	63
	4–3	C7-insol	14	140.6	18.1	2.2	82
5	5–1	EE-sol	8	n/o	n/d	n/d	n/d
	5–2	C7-sol	33	155.3	102.6	2.4	n/d
	5–3	C7-insol	59	155.7	419	3.2	n/d
6	6–1	EE-sol	19	n/o	n/d	n/d	26
	6–2	C7-sol	33	153.2	158	4.8	58
	6–3	C7-insol	48	155.3	160	5.1	85
7	7–1	EE-sol	65	n/o	7.34	2.9	n/d
	7–2	C7-sol	30	143.4	27.0	3.0	n/d
	7–3	C7-insol	5	n/d	49.2	3.7	n/d
8	8–1	EE-sol	90	n/o	2.04	2.1	n/d
	8–2	C7-sol	10	n/d	9.57	2.9	n/d
9	9–1	EE-sol	87	n/o	36.2	2.1	n/d
	9–2	C7-sol	11	155.8	43.6	2.4	n/d
13		EE-sol	100	n/o	15.2	2.1	5.4
17		C7-sol	97	128.7	19.1	2.1	76

[a] Entry numbers correspond to those in Table 1. [b] Determined by ¹³C NMR spectroscopy. [c] Not observed. [d] Not determined.

each extracted portion as described in Scheme 1 and the equilibria are largely affected by temperature. Moreover, it can also be seen that the isospecific active species give higher molecular weight products than the aspecific active species at all temperatures.

In contrast, the polypropylenes from **3-Me**, **4-Me**, and **5-Me**/[Ph₃C][B(C₆F₅)₄] (Table 1, entries 13–15) are completely diethyl ether soluble and atactic with the low *[mmmm]*

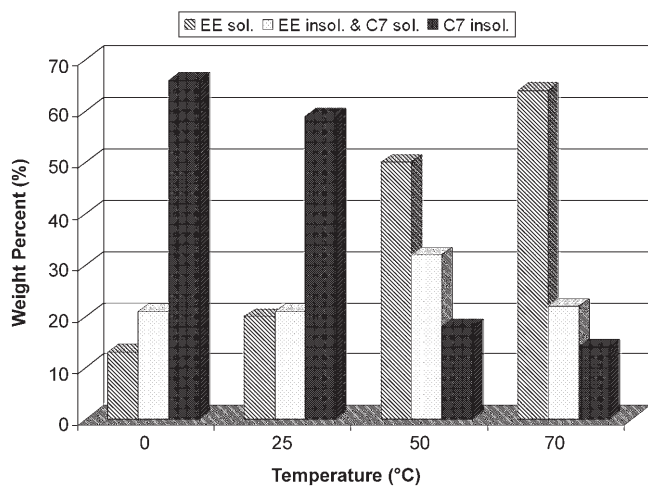


Figure 3. Weight percentage of each extracted fraction from entries 1–4 in Table 1 (**3**/MAO at 0–70°C).

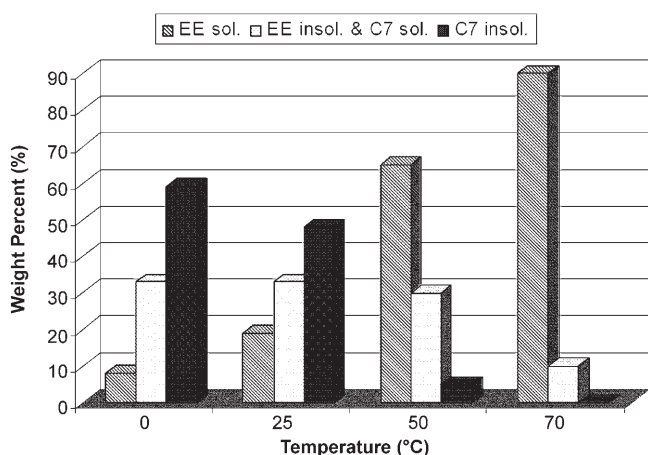


Figure 4. Weight percentage of each extracted fraction from entries 5–8 in Table 1 (**4**/MAO at 0–70°C).

value similar to the result from the aspecific BPZr/MAO system (Table 1, entry 16), indicating essentially no stereocontrol under $[\text{Ph}_2\text{C}][\text{B}(\text{C}_6\text{F}_5)_4]$ activation. The extracted portions of polypropylene from the well-known isospecific catalytic system EBIZr/MAO (Table 1, entry 17), on the other hand, comprise an almost diethyl ether insoluble, but *n*-heptane-soluble portion that corresponds to the $[mmmm]$ value of 76%. The fact that **3**/MAO (Table 2, entry 2) and **4**/MAO (Table 2, entry 6) afforded moderate amounts of *n*-heptane-insoluble portions having the $[mmmm]$ value of 86 and 85%, respectively, under the same condition indicates that the foregoing **3**/MAO and **4**/MAO systems are highly isospecific.

The proposition that the origin of isospecificity is the concurrent working of the cation–anion pairing and the Lewis acid–base interaction between the $[\text{Me-MAO}]^-$ ion and the heteroatom-functionalized unbridged cationic zirconocene species^[28] leads to the expectation that the strength of such

an interaction may play a crucial role in governing isospecificity. When the heteroatom was changed from nitrogen (**3**) to oxygen (**4**), and to sulfur (**5**), the amount of the *n*-heptane-insoluble portion decreased in the order of $\mathbf{3} > \mathbf{4} \gg \mathbf{5}$ at all temperatures. The *n*-heptane-insoluble portion of polymer from **3**/MAO varies from 66 to 59, 18, and 14% as the temperature changes from 0 to 25, 50, and 70°C, whereas **4**/MAO gives the *n*-heptane-insoluble portion of 59, 48, 5, and 0% as the temperature increases, and **5**/MAO produces almost 0% of the *n*-heptane-insoluble portion at all temperatures. These results clearly show that the OMe group, as well as the NMe₂ group, interacts strongly enough with the Lewis acidic sites of the $[\text{Me-MAO}]^-$ ion to attain isospecific propagation of the propylene monomer, whereas the sulfur atom fails to achieve such an interaction in spite of the structural similarity of **5** with **3** and **4**. Although **4**/MAO readily produces an isotactic portion at low temperature (0 and 25°C), the smaller amount than that from **3**/MAO and the sharp decrease with increasing temperature (50 and 70°C) reflect that the Lewis acid–base interaction in **4**/MAO is weaker than that in **3**/MAO. Furthermore, this finding is well correlated with the strength of the interaction of the Lewis acidic metals with N, O, and S atoms.^[33] Therefore, the foregoing demonstration that the Lewis basicity of a functional group affects the isoselectivity of the unbridged class I zirconocene system is supportive of our proposition^[28] with regards to the origin of the isospecificity of heteroatom-functionalized unbridged zirconocenes.

To investigate the effect of monomer concentration on the isospecific polymerization behavior of the above-mentioned catalytic systems, we conducted propylene polymerization experiments under liquid propylene conditions. Since the isospecificity results from an in situ generated, C₂-symmetric-like cation–anion ion pair, the monomer concentration may control the amount of the resulting isotactic portion by changing the rate of monomer insertion in the equilibrium between such an ion pair and the separated aspecific species. Moreover, it was previously revealed that the rate of ligand rotation in **3**/MAO is extremely slow.^[28] It is thus expected that the overall isotactic polypropylene content of the system could be increased as the monomer concentration increases. The polymerization results presented in Table 3 are in good agreement with this hypothesis, and **3** and **4**/MAO indeed afford much increased amounts of highly isotactic polypropylene even at high temperature (Table 3, entries 18–23). Most remarkably, the SMe-substituted **5** that produces negligible amounts of isotactic polypropylene under atmospheric monomer pressure also gives appreciable amounts of a highly isotactic portion (Table 3, entries 24–26). Consistent with this result is the high *T_m* value of all the polypropylenes, and the *T_m* values are still greater than that from EBIZr, indicating higher isotacticity, as similarly observed under atmospheric conditions. In addition, the relative catalytic activity with respect to EBIZr is dramatically increased when compared to that at atmospheric monomer pressure. The increase of an isotactic portion further leads to the increase of overall molecular weight of

Table 3. Propylene polymerization data under liquid propylene condition.^[a]

Entry	Catalyst	T_p [°C]	Pressure [bar]	Yield [g]	Productivity ^[b]	M_w ($\times 10^{-3}$)	M_w/M_n	T_m [°C]	EE-sol wt % ^[c]	EE-insol/C7-sol wt % ^[c]	EE-insol/C7-insol wt % ^[c]
18	3	42	16	45	710	222	7.6	153.4	20	30	50
19	3	60	24	78	1260	170	8.4	152.8	16	23	61
20	3	70	30	102	1610	128	12.2	157.1	17	23	60
21	4	30	13	8.0	130	389	5.9	149.7	17	4	79
22	4	60	24	54	850	233	6.7	151.0	10	28	62
23	4	70	30	54	850	180	9.4	153.9	17	25	58
24	5	30	13	15	240	349	5.0	156.1	13	45	42
25	5	60	24	65	100	144	5.3	157.0	48	39	13
26	5	70	30	82	130	95	6.0	156.0	57	31	12
27 ^[d]	EBIZr	70	30	80	2120	30.3	2.6	130.6	n/d ^[e]	n/d	n/d

[a] Polymerization conditions: propylene monomer = 500 g; [Zr] = 5.0 μmol ; [Al]/[Zr] = 2000. [b] In units of (Kg of PP)(mol of Zr)⁻¹h⁻¹[propylene]⁻¹. [c] EE = diethyl ether; C7 = *n*-heptane. [d] [Zr] = 3.0 μmol . [e] Not determined.

the crude polypropylene. The broad MWD of the obtained polypropylenes at all reaction temperatures indicates the involvement of multiactive species in the bulk polymerization. Since the structurally similar but unfunctionalized catalyst $[\{1-(\text{C}_6\text{H}_5)-3,4\text{-Me}_2\text{C}_5\text{H}_2\}_2\text{ZrCl}_2]$ was reported to afford atactic polypropylene with an almost identical level of $[mmmm]$ content regardless of the monomer concentration,^[19] it can be assumed that the aspecific active species in the form of a completely separated ion pair does not contribute to the increased amount of the isotactic portion; thus, the observed isospecificity is attributed to the in situ generated, C_2 -symmetric-like cation–anion ion pair. The increased rate of monomer insertion upon increasing the monomer concentration, which is evident from a sharp increase of the catalytic activity, most likely results in the increase of the isotactic portion even in a weakly interacting **5**/MAO system and at high temperature.^[34] In addition to the polymerization results from the atmospheric monomer conditions, the present results of bulk polymerizations suggest that the given class of heteroatom-functionalized, unbridged zirconocenes provides a novel strategy for isospecific propylene polymerization.

Conclusion

We have synthesized a set of various Lewis base functionalized unbridged zirconocene complexes **3**, **4**, and **5** and examined their catalytic properties in propylene polymerization under MAO, as well as, $[\text{Ph}_3\text{C}][\text{B}(\text{C}_6\text{F}_5)_4]$ activation. The complexes **3** and **4** that contain nitrogen and oxygen atoms, respectively, showed isospecific propylene polymerization behavior under MAO activation, whereas they gave completely amorphous polypropylene under $[\text{Ph}_3\text{C}][\text{B}(\text{C}_6\text{F}_5)_4]$ at atmospheric monomer pressure. In contrast, the unfunctionalized zirconocene of a similar structure and the SME-substituted **5** gave only atactic polypropylene under both activation conditions. Interestingly, further investigation of the bulk polymerization under liquid propylene showed not only a large increase in an isotactic portion of the obtained polypropylenes, but also the apparent isospecific nature of **4**/MAO and **5**/MAO systems even at high temperature.

These results indicate that the simple Lewis base functionalization of a “class II” unbridged metallocene system into a “class I” system produces an isospecific catalytic system through the in situ generation of rigid *rac*-like cationic active species, the Lewis acid–base interaction of which is dependent upon functionality.

Experimental Section

General considerations: All operations were performed under inert nitrogen gas by using standard Schlenk and glovebox techniques. Anhydrous grade toluene, CH_2Cl_2 , and *n*-hexane (Aldrich) were purified by passing through an activated alumina (Acros, 50–200 μm) column. Anhydrous grade THF (Aldrich) and Et_2O (J.T. Baker) were distilled from Na-benzophenone ketyl. All solvents were stored over activated molecular sieves (5 Å, Yakuri Pure Chemicals Co). Chemicals were used without further purification after purchase from Aldrich (4-bromo-*N,N*-dimethylaniline, 4-methoxyphenylmagnesium bromide, 4-bromothioanisole, polyphosphoric acid, *n*BuLi (2.5 M solution in *n*-hexane), *p*-toluenesulfonic acid (*p*-TsOH), MeLi (1.6 M solution in diethyl ether), triisobutylaluminum (TIBA, 1.0 M in hexanes), and Strem ($[\text{ZrCl}_4(\text{thf})_2]$). 3,4-Dimethylcyclopent-2-enone,^[35] $[\{1-(p\text{-Me}_2\text{NC}_6\text{H}_4)-3,4\text{-Me}_2\text{C}_5\text{H}_2\}_2\text{ZrX}_2]$ (X = Cl (**3**); Me (**3-Me**)),^[28] and $[\{1-(p\text{-C}_6\text{H}_5\text{C}_6\text{H}_4)-3,4\text{-Me}_2\text{C}_5\text{H}_2\}_2\text{ZrCl}_2]$ (BPZr) were prepared according to the literature procedures. CDCl_3 was dried over activated molecular sieves (5 Å) and used after vacuum transfer to a Schlenk tube equipped with a J. Young valve. Methylaluminoxane (MAO) was used as solid MAO obtained by evaporation of the solvent from a solution of PMAO (Witco, 30T) in toluene. The $[\text{Ph}_3\text{C}][\text{B}(\text{C}_6\text{F}_5)_4]$ was used as received (Asahi Glass Co.). Polymerization-grade propylene monomer from the Honam Petrochemical Corporation was used after purification by passing through Labclear and Oxiclear filters. ¹H and ¹³C NMR spectra of compounds were recorded on a Bruker Spectrospin 400 spectrometer at ambient temperature. All chemical shifts are reported in δ units with reference to the residual peaks of CDCl_3 for proton ($\delta = 7.24$ ppm) and carbon ($\delta = 77.0$ ppm) chemical shifts. Elemental analyses were carried out on an EA 1110-FISONS (CE Instruments) at KAIST.

Synthesis of 1-(*p*-MeOC₆H₄)-3,4-Me₂C₅H₃ (1**):** A solution of 3,4-dimethylcyclopent-2-enone (2.20 g, 20 mmol) in THF (20 mL) was slowly added through a cannula at -78°C to a solution of 4-methoxyphenylmagnesium bromide (0.5 M) in THF (40 mL). The reaction mixture was slowly allowed to warm to room temperature and was stirred overnight. The resulting orange solution was treated with saturated aqueous solution of NH_4Cl (50 mL) to quench the reaction. Next, the organic portion was separated and the aqueous layer was further extracted with diethyl ether (50 mL). The combined organic portions were dried over MgSO_4 , filtered, and evaporated to dryness, affording a light orange oily product.

The crude product was redissolved in CH_2Cl_2 (30 mL), and then a catalytic amount of *p*-TsOH (ca. 0.1 g) was added as a solid into the solution at room temperature followed by stirring for about 60 min. After reduction of the volume of the resulting reaction mixture, recrystallization in ethanol at -20°C afforded **1** (2.20 g) in 47% yield. ^1H NMR (400.13 MHz, CDCl_3): $\delta=7.36$ (d, 2H), 6.81 (d, 2H), 6.50 (s, 1H), 3.79 (s, 3H), 3.22 (s, 2H), 1.95 (s, 3H), 1.87 ppm (s, 3H); $^{13}\text{C}\{^1\text{H}\}$ NMR (100.62 MHz, CDCl_3): $\delta=158.1, 142.2, 135.4, 134.7, 129.8, 129.6, 125.7, 113.9, 55.3, 45.3, 13.4, 12.6$ ppm.

Synthesis of 1-(*p*-MeSC₆H₄)-3,4-Me₂C₅H₃ (2): A solution of 4-bromothioanisole (4.33 g, 20 mmol) in diethyl ether (50 mL) was treated with one equivalent of *n*BuLi (8.0 mL) at 0°C . After the mixture had been stirred for 2 h at room temperature, the solvent was evaporated in vacuo, and the obtained white lithium salt was washed with *n*-hexane (2×20 mL). After the addition of THF (40 mL), one equivalent of 3,4-dimethylcyclopent-2-enone (2.20 g, 20 mmol) in THF (20 mL) was slowly added through a cannula at -78°C . The reaction mixture was slowly allowed to warm to room temperature and was stirred overnight. Further work-up and dehydration were carried out in a manner analogous to the procedure for **1**. Recrystallization in ethanol at -20°C afforded **2** (1.69 g) in 39% yield. ^1H NMR (400.13 MHz, CDCl_3): $\delta=7.34$ (d, 2H), 7.17 (d, 2H), 6.61 (s, 1H), 3.22 (s, 2H), 2.46 (s, 3H), 1.96 (s, 3H), 1.87 ppm (s, 3H); $^{13}\text{C}\{^1\text{H}\}$ NMR (100.62 MHz, CDCl_3): $\delta=141.9, 135.7, 135.55, 135.50, 133.6, 131.4, 127.1, 124.9, 45.2, 16.2, 13.4, 12.6$ ppm.

Synthesis of [1-(*p*-MeOC₆H₄)-3,4-Me₂C₅H₃]₂ZrCl₂ (4): A slurry of **1** (1.202 g, 6.0 mmol) in diethyl ether (30 mL) was treated with one equivalent of *n*BuLi (2.4 mL) at -78°C . The reaction mixture was allowed to warm to room temperature and was stirred for 4 h. The resulting reaction mixture was evaporated to dryness, and the lithium salt of **1** was combined with 0.5 equivalents of $[\text{ZrCl}_2(\text{thf})_2]$ (3.0 mmol, 1.132 g). Toluene (50 mL) was then introduced into the solid mixture at -78°C . After allowing to warm to room temperature, the reaction mixture was heated to 50°C and stirred at this temperature overnight. The orange suspension formed was filtered through a Celite pad and the filtrate was evaporated to dryness. Washing with *n*-hexane followed by drying in vacuo afforded **4** (0.891 g) in 53% yield. Light yellow single crystals suitable for X-ray structural determination could be obtained by cooling of a solution of **4** in diethyl ether/*n*-hexane at -20°C . ^1H NMR (400.13 MHz, CDCl_3): $\delta=7.38$ (d, 4H), 6.96 (d, 4H), 6.16 (s, 4H), 3.85 (s, 6H), 1.78 ppm (s, 12H); $^{13}\text{C}\{^1\text{H}\}$ NMR (100.62 MHz, CDCl_3): $\delta=159.0, 127.7, 126.5, 126.1, 122.7, 115.4, 114.5, 55.4, 13.2$ ppm; elemental analysis calcd (%) for $\text{C}_{28}\text{H}_{30}\text{Cl}_2\text{O}_2\text{Zr}$: C 59.98, H 5.39; found: C 59.63, H 5.64.

Synthesis of [1-(*p*-MeSC₆H₄)-3,4-Me₂C₅H₃]₂ZrCl₂ (5): An analogous procedure for **4** was employed by using the ligand **2** (1.298 g, 6.0 mmol) which afforded **5** (0.907 g) as a yellow solid in 51% yield. ^1H NMR (400.13 MHz, CDCl_3): $\delta=7.35$ (d, 4H), 7.30 (d, 4H), 6.20 (s, 4H), 2.51 (s, 6H), 1.79 ppm (s, 12H); $^{13}\text{C}\{^1\text{H}\}$ NMR (100.62 MHz, CDCl_3): $\delta=137.8, 130.1, 128.2, 126.9, 125.6, 122.0, 115.7, 15.8, 13.2$ ppm; elemental analysis calcd (%) for $\text{C}_{28}\text{H}_{30}\text{Cl}_2\text{S}_2\text{Zr}$: C 56.73, H 5.10; found: C 56.21, H 5.36.

Synthesis of [1-(*p*-MeOC₆H₄)-3,4-Me₂C₅H₃]₂ZrMe₂ (4-Me): A slurry of **4** (1.121 g, 2.0 mmol) in diethyl ether (30 mL) was treated with two equivalents of MeLi (2.5 mL) at -78°C . The reaction mixture was allowed to warm to room temperature and was stirred for 4 h. The resulting reaction mixture was evaporated to dryness and extracted with CH_2Cl_2 (30 mL). Filtration followed by evaporation of the solvent gave a yellow residue. Recrystallization from the concentrated CH_2Cl_2 solution layered by *n*-hexane at -20°C afforded **4-Me** (0.613 g) in 59% yield. ^1H NMR (400.13 MHz, CDCl_3): $\delta=7.11$ (d, 4H), 6.86 (d, 4H), 5.57 (s, 4H), 3.82 (s, 6H), 1.81 (s, 12H), -0.49 ppm (s, 6H); $^{13}\text{C}\{^1\text{H}\}$ NMR (100.62 MHz, CDCl_3): $\delta=158.1, 127.8, 125.4, 122.0, 120.5, 114.1, 108.5, 55.3, 30.5, 12.9$ ppm. MS (HR EI): *m/z* calcd for $\text{C}_{30}\text{H}_{36}\text{O}_2\text{Zr}$: 518.1762; found: 518.1758; elemental analysis calcd (%) for $\text{C}_{30}\text{H}_{36}\text{O}_2\text{Zr}$: C 69.32, H 6.98; found: C 67.27, H 6.57.

Synthesis of [1-(*p*-MeSC₆H₄)-3,4-Me₂C₅H₃]₂ZrMe₂ (5-Me): An analogous procedure to that which gave **4-Me** was employed with **5** (1.186 g, 2.0 mmol) to afford **5-Me** (0.440 g) in 40% yield. ^1H NMR (400.13 MHz, CDCl_3): $\delta=7.20$ (d, 4H), 7.07 (d, 4H), 5.62 (s, 4H), 2.49 (s, 6H), 1.82 (s, 12H), -0.49 ppm (s, 6H); $^{13}\text{C}\{^1\text{H}\}$ NMR (100.62 MHz, CDCl_3): $\delta=135.9,$

132.0, 127.0, 124.7, 122.5, 119.8, 108.9, 31.1, 16.1, 12.9; elemental analysis calcd (%) for $\text{C}_{30}\text{H}_{36}\text{S}_2\text{Zr}$: C 65.28, H 6.57, S 11.62; found: C 64.25, H 6.47, S 12.63.

X-ray structure determination of 4: The crystallographic measurement was performed by using a Bruker Apex II-CCD area detector diffractometer, with graphite-monochromated $\text{MoK}\alpha$ radiation ($\lambda=0.71073$ Å). A specimen of suitable size and quality was selected and mounted onto a glass capillary. The structure was solved by direct methods and all non-hydrogen atoms were subjected to anisotropic refinement by full-matrix least-squares on F^2 by using the SHELXTL/PC package. Hydrogen atoms were placed at their geometrically calculated positions and refined riding on the corresponding carbon atoms with isotropic thermal parameters. Final refinement converged at $R1=0.0367$ ($I>2.0\sigma(I)$) and $wR2=0.0974$ (all data). The detailed crystallographic data and selected bond lengths and angles are given in the Supporting Information.

CCDC-642347 (**4**) contains the supplementary crystallographic data for this paper. This data can be obtained free of charge from the Cambridge Crystallographic Data Centre via www.ccdc.cam.ac.uk/data_request/cif.

Propylene polymerization under atmospheric conditions: Freshly distilled toluene (48 mL) was transferred into a well-degassed 250-mL glass reactor charged with a pre-weighed amount of s-MAO ($[\text{Al}]/[\text{Zr}]=1000$), and the temperature was adjusted by using an external bath. After saturation of the propylene monomer at 1 bar with vigorous stirring for 30 min, polymerization was started by the injection of a solution of catalyst (2.0 mL, 5.0 μmol of Zr) in toluene. When $[\text{Ph}_3\text{C}][\text{B}(\text{C}_6\text{F}_5)_4]$ was used as a cocatalyst instead of MAO, the activated catalyst solution (2.0 mL, 5.0 μmol of Zr) was first prepared by treating a dimethyl precursor with an equimolar amount of $[\text{Ph}_3\text{C}][\text{B}(\text{C}_6\text{F}_5)_4]$ in the presence of a measured amount of TIBA ($\text{Al}/\text{Zr}=200$). Next, the polymerization was started by the injection of the solution into the reactor. After 120 min, all the reactions were quenched by the injection of acidified ethanol (5 mL, 10% HCl in EtOH). The resulting polypropylenes were further precipitated by the addition of EtOH (200 mL). After the mixtures had been stirred for 1–2 h, the polypropylenes were collected by filtration or decanting the solution (in the case of a sticky polymer) and were washed with EtOH several times. The resulting polypropylenes were dried in a vacuum oven at 80°C to a constant weight.

Propylene polymerization under liquid propylene conditions: A solution of pre-weighed catalyst (5.0 μmol of Zr) and s-MAO ($[\text{Al}]/[\text{Zr}]=2000$) in toluene (20 mL) was transferred into a well-degassed 2-L stainless-steel reactor charged with nitrogen, and the temperature was adjusted by using a circulator. Polymerization was started by the addition of liquid propylene monomer (500 g). After 60 min, all the reactions were finished by exhausting the remaining propylene monomer. The resulting polypropylenes were precipitated by addition of EtOH (1 L). After the mixtures had been stirred for 1–2 h, the polypropylenes were collected by filtration and were washed with EtOH several times. The resulting polypropylenes were dried in a vacuum oven at 80°C to a constant weight.

Polymer extraction: Solvent extraction of all the polypropylenes was carried out by using a Soxhlet extractor. A pre-weighed polypropylene (1.00 g) was successively extracted with boiling diethyl ether (100 mL) for 12 h. Then, the residue was further extracted with boiling *n*-heptane (100 mL) for another 12 h. Evaporation of the resulting solutions by using a rotary evaporator afforded diethyl ether soluble and diethyl ether insoluble/*n*-heptane-soluble portions of polypropylene, respectively. The obtained portions and the remaining residue (*n*-heptane-insoluble portion) were finally dried under vacuum at 80°C to a constant weight.

Polymer analysis: ^{13}C NMR spectra of polypropylenes were recorded on a Bruker Spectrospin 400 (^{13}C ; 100.62 MHz) for the diethyl ether soluble and diethyl ether insoluble/*n*-heptane-soluble portions at 100°C , and on a Bruker AMAX 500 (^{13}C ; 125.77 MHz) spectrometer for the *n*-heptane-insoluble portions at 120°C with a 90° pulse angle, an acquisition time of 2 s, and a relaxation delay of 8 s. The samples were dissolved in 1,1,2,2-[D₂]tetrachloroethane to form a 10 wt % solution (about 90 mg/0.5 mL) in 5 mm tubes. All the measurements were performed after complete dissolution by warming (for the diethyl ether soluble and diethyl ether insoluble/*n*-heptane-soluble portions) or pre-heating (for the *n*-heptane-insoluble portions) to about 110°C in an oil bath. The chemical shift value

of the residual peak of the solvent ($\delta=74.14$ ppm) was used as an internal standard. Peak assignments and the determination of the methyl pentad sequence distributions were made according to the reported literature.^[4] Molecular weight (M_w) and molecular weight distributions (M_w/M_n) of polypropylenes were determined by gel-permeation chromatography (GPC, Polymer Laboratories PL-GPC 220, 140°C) in 1,2,4-trichlorobenzene by using standard polystyrenes as a reference. Melting temperatures (T_m) of polypropylenes were measured by differential scanning calorimetry (DSC, TA Instrument 2910 MDSC) at a heating rate of 10°Cmin⁻¹. Any thermal history in the polymers was eliminated by first heating the samples to 180°C at 20°Cmin⁻¹, cooling to 30°C at 20°Cmin⁻¹, and then recording the second DSC scan from 30 to 180°C.

Acknowledgements

The authors gratefully acknowledge financial support from CMDS-(KOSEF), POMRC, and the BK-21 project. We also thank Honam Petrochemical Co. for GPC and DSC analyses and the donation of fresh monomer.

- [1] S. D. Ittel, L. K. Johnson, M. Brookhart, *Chem. Rev.* **2000**, *100*, 1169.
 [2] H. G. Alt, A. Köppl, *Chem. Rev.* **2000**, *100*, 1205.
 [3] G. W. Coates, *Chem. Rev.* **2000**, *100*, 1223.
 [4] L. Resconi, L. Cavallo, A. Fait, F. Piemontesi, *Chem. Rev.* **2000**, *100*, 1253.
 [5] S. Park, Y. Han, S. K. Kim, J. Lee, H. K. Kim, Y. Do, *J. Organomet. Chem.* **2004**, *689*, 4263.
 [6] V. C. Gibson, S. K. Spitzmesser, *Chem. Rev.* **2003**, *103*, 283.
 [7] W. Kaminsky, *Adv. Catal.* **2001**, *46*, 89.
 [8] G. J. P. Britovsek, V. C. Gibson, D. F. Wass, *Angew. Chem.* **1999**, *111*, 448; *Angew. Chem. Int. Ed.* **1999**, *38*, 428.
 [9] H. H. Brintzinger, D. Fischer, R. Mülhaupt, B. Rieger, R. M. Waymouth, *Angew. Chem.* **1995**, *107*, 1255; *Angew. Chem. Int. Ed. Engl.* **1995**, *34*, 1143.
 [10] J. A. Ewen, *Macromol. Symp.* **1995**, *89*, 181.
 [11] J. A. Ewen, *J. Am. Chem. Soc.* **1984**, *106*, 6355.
 [12] J. A. Ewen, R. L. Jones, A. Razavi, *J. Am. Chem. Soc.* **1988**, *110*, 6255.
 [13] S. A. Miller, J. E. Bercaw, *Organometallics* **2004**, *23*, 1777.
 [14] G. Erker, R. Nolte, R. Aul, S. Wilker, C. Krüger, R. Noe, *J. Am. Chem. Soc.* **1991**, *113*, 7594.
 [15] G. Erker, B. Temme, *J. Am. Chem. Soc.* **1992**, *114*, 4004.
 [16] G. Erker, M. Aulbach, M. Knickmeier, D. Wingbermühle, C. Krüger, M. Nolte, S. Wener, *J. Am. Chem. Soc.* **1993**, *115*, 4590.
 [17] G. Coates, R. M. Waymouth, *Science* **1995**, *267*, 217.
 [18] E. Hauptman, R. M. Waymouth, J. W. Ziller, *J. Am. Chem. Soc.* **1995**, *117*, 11586.
 [19] J. L. Maciejewski Petoff, M. D. Bruce, R. M. Waymouth, A. Masood, T. K. Lal, R. W. Quan, S. J. Behrend, *Organometallics* **1997**, *16*, 5909.
 [20] J. L. Petoff, C. L. Myers, R. M. Waymouth, *Macromolecules* **1999**, *32*, 7984.
 [21] S. Lin, C. D. Tagge, R. M. Waymouth, M. Nele, S. Sollins, J. C. Pinto, *J. Am. Chem. Soc.* **2000**, *122*, 11275.
 [22] S. Lin, R. M. Waymouth, *Acc. Chem. Res.* **2002**, *35*, 765.
 [23] G. M. Wilmes, J. L. Polse, R. M. Waymouth, *Macromolecules* **2002**, *35*, 6766.
 [24] V. Busico, R. Cipullo, W. P. Kretschmer, G. Talarico, M. Vacatello, V. V. A. Castelli, *Angew. Chem.* **2002**, *114*, 523; *Angew. Chem. Int. Ed.* **2002**, *41*, 505.
 [25] V. Busico, V. V. A. Castelli, P. Aprea, R. Cipullo, A. Segre, G. Talarico, M. Vacatello, *J. Am. Chem. Soc.* **2003**, *125*, 5451.
 [26] A. L. Lincoln, G. M. Wilmes, R. M. Waymouth, *Organometallics* **2005**, *24*, 5828.
 [27] M. H. Lee, Y. Do, *J. Organomet. Chem.* **2005**, *690*, 1240.
 [28] S. K. Kim, H. K. Kim, M. H. Lee, S. W. Yoon, Y. Do, *Angew. Chem.* **2006**, *118*, 6309; *Angew. Chem. Int. Ed.* **2006**, *45*, 6163.
 [29] K. Kimura, K. Takaishi, T. Matsukawa, T. Yoshimura, H. Yamazaki, *Chem. Lett.* **1998**, 571.
 [30] 2,1-Regioerrors, which could also contribute to the comparatively broad polydispersities by producing less reactive sites that favor chain-transfer reactions, were hardly detected with our routine NMR parameters, thus indicating that the influence of the regioselectivity on polydispersity may not be significant in this system.
 [31] M. Atiqullah, H. Hammawa, H. Hamid, *Eur. Polym. J.* **1998**, *34*, 1511.
 [32] A. Lehtinen, R. Paukeri, *Macromol. Chem. Phys.* **1994**, *195*, 1539.
 [33] R. S. Drago, D. C. Ferris, N. Wong, *J. Am. Chem. Soc.* **1990**, *112*, 8953.
 [34] L. Resconi, A. Fait, F. Piemontesi, M. Colonna, H. Rychlicki, R. Zeigler, *Macromolecules* **1995**, *28*, 6667.
 [35] J. M. Conia, M. L. Leriverend, *Bull. Soc. Chim. Fr.* **1970**, 2981.

Received: April 3, 2007
 Published online: August 3, 2007